European Journal of Radiology 178 (2024) 111620

Contents lists available at ScienceDirect

European Journal of Radiology

journal homepage: www.elsevier.com/locate/ejrad

Research article

# A pilot study to identify suitable MRI protocols for preoperative planning of total hip arthroplasty

Switinder Singh Ghotra [a,b,*], Yann Cottier [c], Christine Bruguier [d,e], Alejandro Dominguez [a,e], Pascal Monnin [a], Cláudia Sá dos Reis [a]

[a] School of Health Sciences (HESAV), University of Applied Sciences and Arts Western Switzerland (HES-SO), Lausanne 1011, Switzerland
[b] Department of Radiology, Hospital of Yverdon-les-Bains (eHnv), 1400 Yverdon-les-Bains, Switzerland
[c] Centre d'Imagerie Diagnostique de Lausanne, Lausanne 1011, Switzerland
[d] Department of Diagnostic & Interventional Radiology, Lausanne University Hospital (CHUV) and University of Lausanne (UNIL), Lausanne 1011, Switzerland
[e] University Center of Legal Medicine Lausanne – Geneva, Lausanne University Hospital (CHUV) and University of Lausanne (UNIL), Lausanne 1011, Switzerland

ARTICLE INFO

*Keywords:*
Musculoskeletal system
Magnetic resonance imaging
Visual grading analysis
Turbo spin echo
Gradient echo

ABSTRACT

*Purpose:* The purpose of this study is to identify suitable MRI sequences and evaluate the feasibility and performance of MRI for total hip arthroplasty (THA) preoperative planning.
*Method:* A multicentric pilot study was conducted to evaluate DP TSE and T1 GRE 3D sequences. High-resolution pelvis, hip, knee and ankle images were acquired. Protocols were optimised to enhance image quality (IQ) and reduce acquisition time to fit clinical practice. The final protocol was validated with 19 healthy volunteers with variable BMIs at 1.5 and 3 Tesla. Visual assessment was performed by five radiographers and radiologists using the ViewDEX software. Visual Grading Analysis (VGA), Intraclass Correlation Coefficient (ICC), Prevalence-adjusted and bias-adjusted kappa (PABAK) and Visual Grading Characteristics (VGC) were performed to analyse data.
*Results:* VGA scores indicated that the optimised 3D DP TSE and 3D T1 GRE sequences at 3 T, as well as 3D DP TSE sequence at 1.5 T offer adequate IQ and allow a correct visualisation of the anatomy. Overall ICC analysis was moderate to good reliability at 0.749 (95 % CI 0.69–0.79) and increased from good to excellent at 0.846 (95 % CI 0.72–0.91) for DP at 3 T. PABAK shows fair agreement at 0.25 (95 % CI 0.227–0.273). VGC analysis showed that 3D DP TSE sequences performed statistically better than 3D T1 GRE at 1.5 and 3 T (p-value $\leq$ 0.05). Furthermore, 3 T sequences showed a statistically better performance compared to 1.5 T (p-value $\leq$ 0.05).
*Conclusions:* According to the results, 3D DP and T1 MRI sequences can be considered for preoperative planning for THA. Further research is required to emphasize the clinical validation of the results.

## 1. Introduction

Total hip arthroplasty (THA) is typically a surgery considered for elderly people due to the development of osteoarthritis. Nevertheless, the need for this surgery is increasing and shifting to a younger population, mainly due to sports and related injuries and also due to a high body mass index (BMI) since it causes additional stress over the joints. Individuals with higher BMI levels are at an increased risk of developing joint-related conditions, such as osteoarthritis mainly on hips and knees [1–3], requiring interventions to improve quality of life. Simultaneously, THA has been documented in very young populations as a consequence of diseases like juvenile idiopathic arthritis and childhood hip diseases [4]. Preoperative planning is known to be fundamental to increase successful outcomes and better quality of life for patients by reducing intraoperative and postoperative complications. Currently, conventional radiography (CR) and Computed Tomography (CT) are being used as preoperative planning tools. However, three-dimensional (3D) pre-operative planning in THA is being presented as a useful tool in planning elective surgery, due to a better definition of the optimal component size, position, and orientation [5]. Also, CT has

* Corresponding author at: School of Health Sciences (HESAV), University of Applied Sciences and Arts Western Switzerland (HES-SO), Lausanne 1011, Switzerland.
*E-mail addresses:* switindersingh.ghotra@hesav.ch (S.S. Ghotra), christine.bruguier@chuv.ch (C. Bruguier), alejandro.dominguez@hesav.ch (A. Dominguez), pascal.monnin@hesav.ch (P. Monnin), claudia.sadosreis@hesav.ch (C. Sá dos Reis).

https://doi.org/10.1016/j.ejrad.2024.111620
Received 3 October 2023; Received in revised form 15 June 2024; Accepted 11 July 2024
Available online 14 July 2024

proven to have a higher accuracy in analysing the hip rotation centre and femoral offset, promoting better surgery outcomes due to the increased preoperative planning accuracy [6–8]. However, CT leads to an increase of ionising radiation in the pelvic area of the patient, exposing the patient to a higher risk of cell damage, especially in a younger population since they have higher radiosensitivity. Principles such as JOLi (Justification, Optimisation and Limitation) and ALARA (As Low As Reasonably Achievable) should be followed and ionising radiation should be avoided if possible [9]. The lower contrast resolution of CT and radiography and the low accuracy of plain radiography are limitations that can be overcome by using Magnetic Resonance Imaging (MRI) examinations. Moreover, CT and MRI images could result in the evaluation of the range of motion [10]. Currently, MRI is already usable as an imaging modality for preoperative planning of knee surgery, which requires similar imaging of the same anatomical areas [15], but it is not fully exploited for THA. Main reasons are due to the acquisition time required, the associated costs and bone density information requirements, even if it is a solution to reduce the radiation exposure [11]. Bone density cartography can be obtained with a MRI in a similar way as in radiation therapy MRI treatment planning [12]. Furthermore, different MRI techniques allow to theoretically meet the THA image quality (IQ) and technical requirements, such as resolution and adequate contrast between cortical and trabecular bone for prosthesis sizing [13,14]. Despite a careful review of the literature on the subject, the question remains unanswered concerning a possible implication of MRI for THA preoperative planning.

The purpose of this study is to identify suitable MRI sequences and evaluate the feasibility and performance of MRI for 3D THA preoperative planning. It aims to assess if MRI images can reproduce adequately for different users the anatomical hip landmarks required for surgery.

## 2. Material and methods

A multicentric pilot study was conducted in three steps to evaluate optimised MRI sequences to meet THA preoperative planning requirements: 1. Image acquisition, 2. Perceptual image assessment and 3. Data analysis.

Study data were acquired prospectively after informing and obtaining written consent from each volunteer participant, in accordance with the ethical principles. All data were anonymous, safely stored in a secured server with limited access and have been managed in compliance with the General Data Protection Regulation (GDPR). Ethical approval for this study has been granted by the Ethics Committee Vaud (CER-VD, Project-ID: 2021–0037).

Once volunteers confirmed their interest, the study information and consent form were given to them, and a screening was performed to verify if they fit the inclusion criteria (Table 1). Before the image acquisition, a session was organised with each volunteer to clarify the procedure and to fill the security forms.

### 2.1. Image acquisition

Right hip images were acquired in 19 healthy volunteers aging from 18 to 60 years with variable BMIs. MRI images were acquired on 1.5 T Philips-Ingenia (Philips Healthcare, Eindhoven, the Netherlands) and on 3 T Siemens Skyra (Siemens-Healthinneers, Erlangen, Germany). Body, torso and table coils were used allowing to move the table to the region of interest in the middle of the field without moving the patient. Peripheral angio 36 coil was used only on the 3 T machine. The knee and ankle coils were removed to maintain lower limb neutral position. Three-Dimensional T1-Weighted Gradient-Echo (3D T1 GRE) and DP-weighted Turbo Spin Echo (3D DP TSE) high-resolution sequences of pelvis, knee, ankle (1 mm3), and hip (0.6 mm3) were acquired at 1,5 and 3 Tesla. These two sequences were optimized in terms of high-resolution capabilities, acquisition time and signal-to-noise ratio (SNR) [13,14]. Protocols were optimised by increasing the parallel imaging factor, balancing the acquired reference line to reduce acquisition time with parallel imaging and avoid aliasing artefact and noise enhancement, applying interpolation between acquired and reconstructed matrix to increase resolution and reduce acquisition time, increasing the number of excitation (NEX) to improve SNR to compensate signal loss related to high-resolution images, band saturation on abdominal fat and artefact reduction to enhance IQ and reduce time to fit clinical practice requirements [15–17] (Table 2). The final protocol was validated with the volunteers.

**Table 1**
Inclusion and exclusion criteria applicable to the participants.

| Inclusion Criteria | Exclusion Criteria |
|---|---|
| – 18 to 60 years old | – Pelvis and/or right limb pathology history |
| – Both genders | – MRI contraindication |
| – Available in the geographic area | – Claustrophobia |
| – Consent form signed | – Difficult to remain still |
| – French, English, German or Italian speaker | – No clear consent |
| | – Pregnancy |

### 2.2. Visual grading analysis

Two authors evaluated all the images acquired from the 19 volunteers (76 stacks), and selected 21 stacks representative of the full sample (BMI, age, gender) which were assessed by 5 observers (3 MRI-experienced radiographers and 2 radiologists). One stack of images was assessed twice to evaluate the reliability.

To evaluate the visibility of anatomical structures and IQ, the ViewDEX software [18–20] was used, which allows absolute Visual Grading Analysis (VGA). Prior to the assessment, the setting was tested and suggestions of improvement were included when relevant [21–23].

The anatomical criteria subject to evaluation were based in the literature [7,24–26] (Table 3). Five criteria were integrated to grade the IQ and evaluate the presence of artefact or deformation [27]. Observers graded the images using an absolute rating scale of 4-point Likert scale and they were asked to state if any artefact or image deformation affected the relevant anatomy using a closed ended question (Table 3). All observers were asked to sit at 1 m from the display system. The display parameters (zoom in/out, window level/width) were set to ensure optimal visualisation conditions.

The clinical setting was prepared considering the references for environmental light and noise [21].

### 2.3. Data analysis

To evaluate if the images offer good quality of the anatomical structures for preoperative planning, mean score of the observers' answers was calculated. The score for each anatomical criteria needed to be greater or equal to 2.5 to answer clinical requirements, while the score for each IQ criteria needed to be greater or equal to 2, as the IQ required is to plan a prosthesis and not for diagnostic purposes [21]. The performance of observer IQ measurements was assessed by intra-class correlation coefficient (ICC). The ICC was used for quantitative data and the 95 % interval confidence (IC) was calculated with and reported as indicated by Koo & all [28]. Furthermore, intra-observer evaluation agreement of IQ was assessed using Prevalence-adjusted and bias-adjusted kappa (PABAK), which reduces bias related to prevalence [29], and interpreted according to Landis and Koch [30]. Stata 15 software (Stats Corp., Texas, USA, 2017) was used to perform statistical analysis. Visual Grading Characteristics (VGC) consist in treating the scale steps as ordinal with no assumptions on the distribution of the data. This allows to take in consideration if observers consistently rate a sequence higher than other [21,22,31]. VGC was performed using VGC Analyser software [32–34]. The Area Under the Curve ($AUC_{VGC}$) is considered as a measure of the difference in IQ between two techniques.

**Table 2**
MRI Acquisition parameters for both equipment 1.5 T and 3 T.

| Imaging parameters | Pelvis DP TSE 3D | | Hip DP TSE 3D | | Hip T1 GRE 3D | | Knee DP TSE 3D | | Ankle DP TSE 3D | |
|---|---|---|---|---|---|---|---|---|---|---|
| | 3 T | 1.5 T | 3 T | 1.5 T | 3 T | 1.5 T | 3 T | 1.5 T | 3 T | 1.5 T |
| TR repetition time (msec) | 1100 | 1100 | 1100 | 1100 | 6 | 7.9 | 1100 | 1100 | 1100 | 1100 |
| TE echo time (msec) | 40 | 25 | 43 | 25 | 2.46 | 3.5 | 40 | 23 | 40 | 23 |
| Flip angle | Variable | Variable | Variable | Variable | 10 | 10 | Variable | Variable | Variable | Variable |
| No. of slices reconstructed | 224 | 210 | 288 | 350 | 256 | 350 | 192 | 200 | 192 | 200 |
| Slice thickness (mm) | 1 | 1 | 0.6 | 0.6 | 0.6 | 0.6 | 1 | 1 | 1 | 1 |
| Field of View ($mm^2$) | 402 × 384 | 410 × 410 | 270 × 271 | 240 × 240 | 250 × 259 | 240 × 240 | 320 × 176 | 245 × 245 | 320 × 176 | 245 × 245 |
| Acquisition matri × | 402 × 384 | 412 × 412 | 448 × 337 | 300 × 300 | 416 × 342 | 300 × 300 | 320 × 176 | 244 × 246 | 320 × 176 | 244 × 246 |
| Pixel spacing ($mm^2$) | 1 × 1 | 1 × 1 | 0.8 × 0.8 | 0.8 × 0.8 | 0.8 × 0.8 | 0.8 × 0.8 | 1 × 1 | 1 × 1 | 1 × 1 | 1 × 1 |
| Reconstructed Voxel size ($mm^3$) | 1 × 1 × 1 | 1 × 1 × 1 | 0.6 × 0.6 × 0.6 | 0.6 × 0.6 × 0.6 | 0.6 × 0.6 × 0.6 | 0.6 × 0.6 × 0.6 | 1 × 1 × 1 | 1 × 1 × 1 | 1 × 1 × 1 | 1 × 1 × 1 |
| Fourier plan sampling | 100 % | 78 % | 75 % | 78 % | 75 % | 100 % | 100 % | 79 % | 100 % | 79 % |
| Coding direction | COR | COR | COR | COR | COR | COR | COR | COR | COR | COR |
| Encoding phases | RL | RL | HF | RL | RL | RL | RL | RL | RL | RL |
| Encoding phases 3D | AP | AP | AP | AP | AP | AP | AP | AP | AP | AP |
| Parallel imaging | GRAPPA | SENSE | GRAPPA | SENSE | GRAPPA | SENSE | GRAPPA | SENSE | GRAPPA | SENSE |
| Parallel imaging factor | 3 | 2.5 RL 1.5 AP | 2 | 2.5 RL 1.5 AP | 2 | 3.2 RL 1.3 AP | 3 | 3 RL 2 AP | 3 | 3 RL 2 AP |
| Turbo factor | 76 | 71 | 46 | 71 | 1 | 27 | 76 | 80 | 76 | 80 |
| Number of excitations | 1 | 1 | 1 | 1 | 1 | 6 | 1 | 1 | 1 | 1 |
| Bandwidth | 450 | 482 | 445 | 524 | 300 | 217 | 445 | 569 | 445 | 569 |
| Time of acquisition (min) | 05:10 | 03:20 | 09:10 | 05:49 | 05:33 | 17:16 | 03:56 | 03:30 | 03:56 | 03:30 |

**Table 3**
Setting (anatomical, image quality, artifacts, deformation) used for visual assessment and Likert-scales.

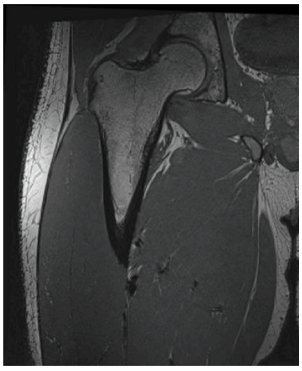

| Right Hip MRI | | | | | |
|---|---|---|---|---|---|
| **Anatomical criteria** | | | | | |
| 1 | The acetabulum is: | 1 | 2 | 3 | 4 |
| 2 | The femoral head is: | 1 | 2 | 3 | 4 |
| 3 | The femoral neck is: | 1 | 2 | 3 | 4 |
| 4 | The greater trochanter is: | 1 | 2 | 3 | 4 |
| 5 | The lesser trochanter is: | 1 | 2 | 3 | 4 |
| 6 | The differentiation between the trabecular and cortical bone is: | 1 | 2 | 3 | 4 |
| **Image quality criteria** | | | | | |
| 7 | The general image quality is: | 1 | 2 | 3 | 4 |
| 8 | The noise is: | 1 | 2 | 3 | 4 |
| 9 | The contrast is: | 1 | 2 | 3 | 4 |
| **Artifact and deformation** | | | | | |
| 10 | Is the relevant anatomy hidden by artifact? | Yes | | No | |
| 11 | Does image deformation alter important anatomy structure? | Yes | | No | |

**Anatomical criteria** (1-6) are assessed with a Likert scale 1 to 4: 1 “not defined”; 2 “slightly defined”; 3 “defined”; 4 “clearly defined”
**Image quality criteria** (7-9) are assessed with a Likert scale 1 to 4: 1 “very poor”; 2 “poor”; 3 “adequate”; 4 “very good”
**Artifact and deformation** problem for relevant anatomy (7-9) are assessed with a closed question “yes” or “no”

A VGC curve situated on or near the diagonal with an $AUC_{VGC}$ value of 0.5 indicates that two sequences produce identical IQ. A greater $AUC_{VGC}$ (>0.5) indicates better IQ for the technique on the vertical axis (test condition), a lesser $AUC_{VGC}$ (<0.5) indicates a superior IQ for the technique on the horizontal axis (reference condition) (22,31). The VGC Analyser software was used to compare the T1 to DP sequence both at 1.5 and 3 T. Interval Confidence (CI) was calculated as well as p-value (0.05), both are required to state statistical significance. If the 95 % IC $AUC_{VGC}$ includes 0.5, it means that there is no significant difference between sequences.

## 3. Results

### 3.1. Participants characteristics

The characteristics of the participants were variable, 7 men and 12 women were enrolled for this study, with an age ranging from 23 to 59, weight between 52 and 92 kg, height between 163 and 197 cm, BMI between 17.78 and 29.03 (Table 4). Four sequences were acquired for each participant (Fig. 1). THA is mainly performed in the elderly population. However, to reduce variability and the impact of pathology on image quality and anatomical reproduction, for this pilot study, only healthy volunteers were included.

### 3.2. Visual grading analysis

VGA scores obtained indicated that the 3D DP TSE and 3D T1 GRE sequences at 3 T, as well as 3D DP TSE sequence at 1.5 T reached the minimum grading of 2.5 for the anatomical reproduction required for preoperative planning of THA (Fig. 2, Fig. 3), while T1 GRE sequences acquired at 1.5 T did not reach the anatomical reproduction of femoral head (2.4) and the lesser trochanter (2.36) (Fig. 2). The 4 sequences

**Table 4**
Participants' characteristics.

| | Gender | Age (years) | Weight (kg) | Height (cm) | BMI |
|---|---|---|---|---|---|
| Participants | 7 Men 12 Women | 23 to 59 | 52 to 92 | 163 to 197 | 17.78 to 29.03 |
| Mean | | 34.4 | 64.6 | 167.95 | 22.59 |
| Participant 1 | male | 28 | 84 | 187 | 24.02 |
| Participant 2 | female | 30 | 75 | 167 | 26.89 |
| Participant 3 | female | 43 | 59.5 | 166 | 27.77 |
| Participant 4 | male | 45 | 60 | 176 | 20.17 |
| Participant 5 | male | 54 | 92 | 178 | 29.03 |

tested reached the minimum grading for IQ fixed at 2. DP TSE sequences were graded higher than T1 GRE sequences for IQ, both at 1.5 and 3 T (Fig. 2, Fig. 3). 3 T sequences offer an overall better anatomical reproduction and IQ compared to 1.5 T sequences (Fig. 4). However, femoral neck and greater troch were graded better at 1.5 than 3 T, while lesser trochanter was not well reproduced at 1.5 compared to 3 T (Fig. 4).

ICC analysis showed an overall moderate to good general agreement between observers at 0.749 (95 % CI 0.69–0.79), while for the DP at 3 T the agreement between observers was good to excellent at 0.846 (95 % CI 0.72–0.91). Additionally, ICC was lower for 1.5 T sequences (Table 5).

PABAK showed a fair agreement of 0.25 (95 % CI 0.227–0.273) for overall grading made in this study by the observers, while VGC analysis indicated that the 3D DP TSE sequences performed statistically better than 3D T1 GRE at 1.5 T for an $AUC_{VGC}$ of 0.61 with a 95 % CI (0.67–0.55), as well at 3 T $AUC_{VGC}$ of 0.72 with a 95 % CI (0.78–0.65) (p-value $\leq$ 0.05). 3 T sequences displayed a statistically better performance compared to 1.5 T sequences (p-value $\leq$ 0.05) for an $AUC_{VGC}$ of 0.63 with a 95 % CI (0.59–0.68) (Fig. 5).

## 4. Discussion

The purpose of this study was to evaluate the feasibility and performance of 3D MRI sequences for THA preoperative planning. The sequences tested in this study were chosen for their capacity to reproduce the anatomical structure and shorten the acquisition time. DP weighting was chosen due to the ability to allow for higher signal acquisition, which is important to allow high-resolution images with lower acquisition time. Furthermore, DP sequences allow for optimal contrast differentiation between fluid and cartilage in joints. In this study, T1 weighting was chosen due to the ability to allow shorter acquisition time and anatomical reproduction ability. T2 weighting sequences were avoided as they have a longer acquisition time and have high signals of fluid, which are not interesting for THA. Fluid signals could hinder correct bone structure reproduction and add artefacts. Furthermore, 3D sequences were selected, which reduced the choice of sequences available to turbo spin echo 3D sequences (SPACE and VISTA) and turbo echo gradient sequences (VIBE and Thrive). Ultrashort echo time (UTE) and Zero echo time (ZTE) sequences seem to be promising for imaging the bone structures, however, they were not available during the study and should investigated in future studies. 3D MRI allows to avoid ionising

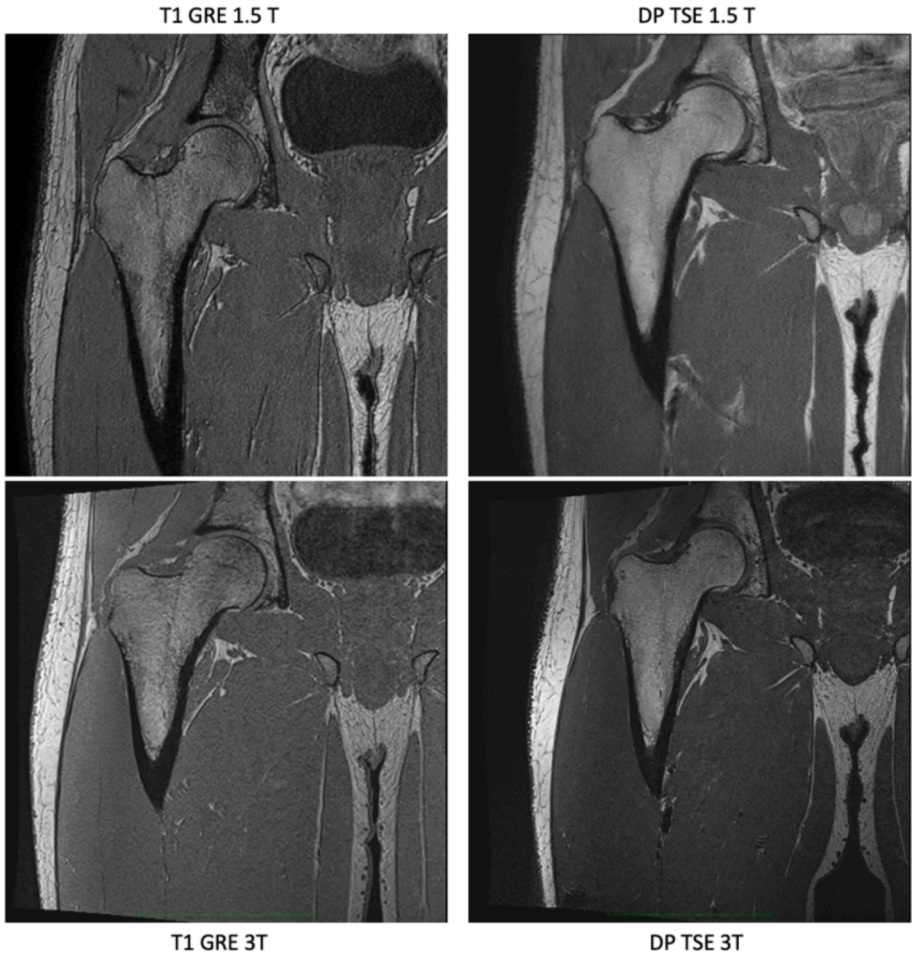


**Fig. 1.** Sequences acquired at 1.5 T and 3 T for each participant.

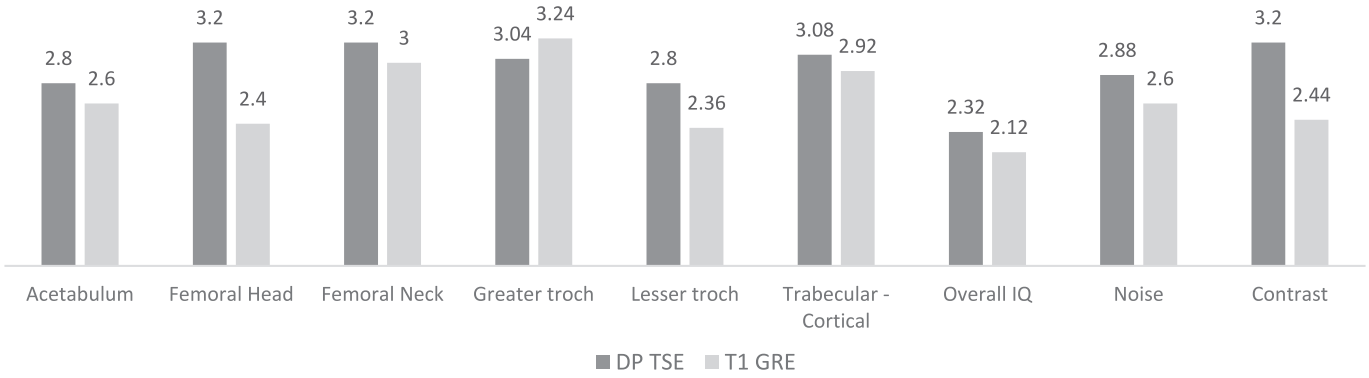


**Fig. 2.** Anatomical and IQ mean at 1.5 T.

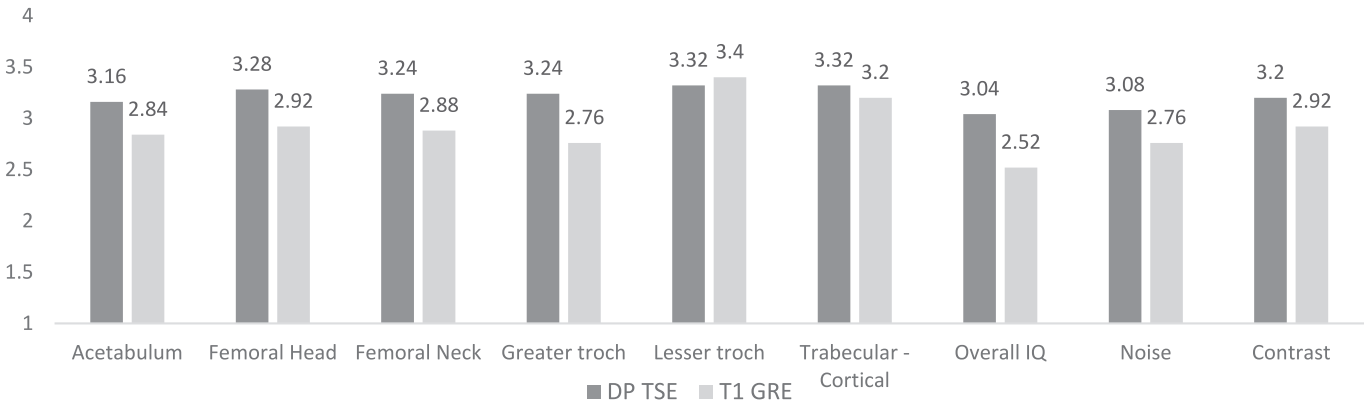


**Fig. 3.** Anatomical and IQ mean at 3 T.

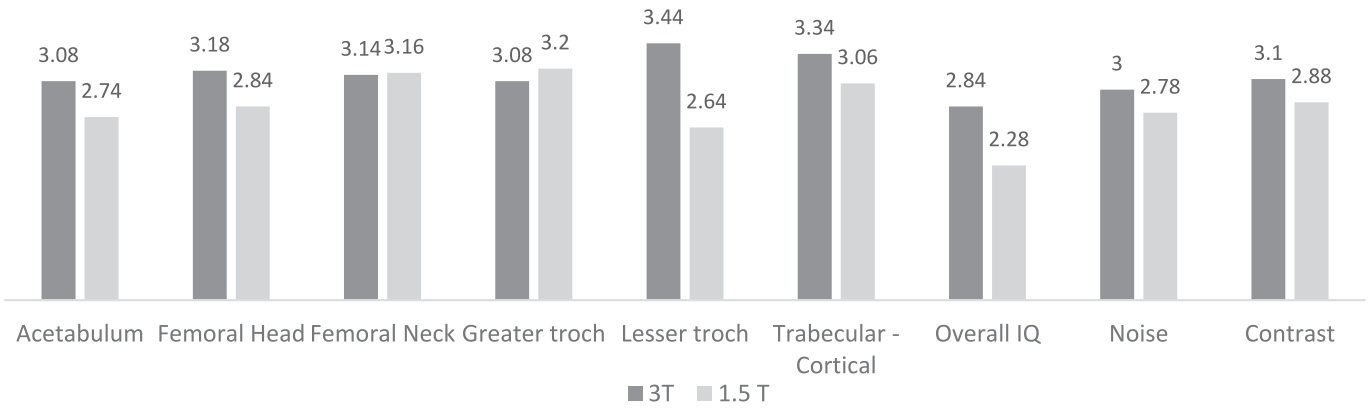


**Fig. 4.** Anatomical and IQ mean at 1.5 T and 3 T.

radiation concerns, to obtain CT-like images for bone density information [12,35], investigation of the soft tissues such as cartilage, tendons and ligaments to assess the biomechanics of the hip joint, as well as the range of motion of the hip, which is fundamental to reinstate the full mobility [10,36,37]. The results indicated that the best sequence to reproduce anatomy references required for THA preoperative planning is 3D DP TSE at 3 T, followed 3D T1 GRE sequences at 3 T. Finally, 3D DP TSE sequence at 1.5 T is also adequate but resulted in the lowest rating. Only the T1 GRE sequence acquired at 1.5 T resulted in insufficient anatomy reproduction. Similar to a previous study, a drastic reduction of IQ impact the anatomical reproduction when the field strength is reduced with high-resolution sequences [38]. Moreover, a GRE sequence has a reduced SNR compared to TSE sequence due the absence of the 180° refocusing pulse [39]. It is possible to increase the SNR by increasing the number of excitations, which also increase proportionally the acquisition time. A possible solution could be the implementation of AI tools to enhance IQ by denoising or increasing resolution and reduce acquisition time rather than relying on number of excitations to increase the SNR [40–42]. 3 T sequences offer an overall better anatomical visualisation and IQ compared to 1.5 T sequences (Fig. 4). Femoral neck and greater troch anatomical reproduction was graded better at 1.5 than 3 T, while lesser trochanter was not well reproduced at 1.5 compared to 3 T (Fig. 4). This is probably related to participants position difference between 1.5 and 3 T. At 1.5 T Philips, patient lower limbs were internally rotated and taped to maintain position, while this was not possible with the peripheral angio 36 coil of Siemens at 3 T. Internal rotation of lower limbs allows “to open” the femoral neck and better visualise the greater trochanter, while slightly reducing the lesser trochanter

**Table 5**
Intra-class Correlation Coefficient (ICC).

| Criteria | Type of agreement | ICC | Interval Confidence | | ICC interpretation |
|---|---|---|---|---|---|
| All criteria | Absolute | 0.708 | 0.618 | 0.777 | Moderate to good |
| | Consistency | 0.749 | 0.692 | 0.79 | Moderate to good |
| DP TSE 3 T | Absolute | 0.819 | 0.721 | 0.887 | Moderate to good |
| | Consistency | 0.846 | 0.771 | 0.902 | Good to Excellent |
| T1 GRE 3 T | Absolute | 0.632 | 0.401 | 0.779 | Poor to moderate |
| | Consistency | 0.742 | 0.616 | 0.836 | Moderate to good |
| DP TSE 1.5 T | Absolute | 0.635 | 0.455 | 0.767 | Poor to good |
| | Consistency | 0.682 | 0.527 | 0.798 | Moderate to good |
| T1 GRE 1.5 T | Absolute | 0.574 | 0.361 | 0.729 | Poor to moderate |
| | Consistency | 0.650 | 0.479 | 0.777 | Poor to good |
| 3 T Criteria | Absolute | 0.756 | 0.629 | 0.837 | Moderate to good |
| | Consistency | 0.814 | 0.753 | 0.863 | Moderate to good |
| 1.5 Criteria | Absolute | 0.622 | 0.486 | 0.727 | Poor to moderate |
| | Consistency | 0.668 | 0.559 | 0.757 | Moderate to good |

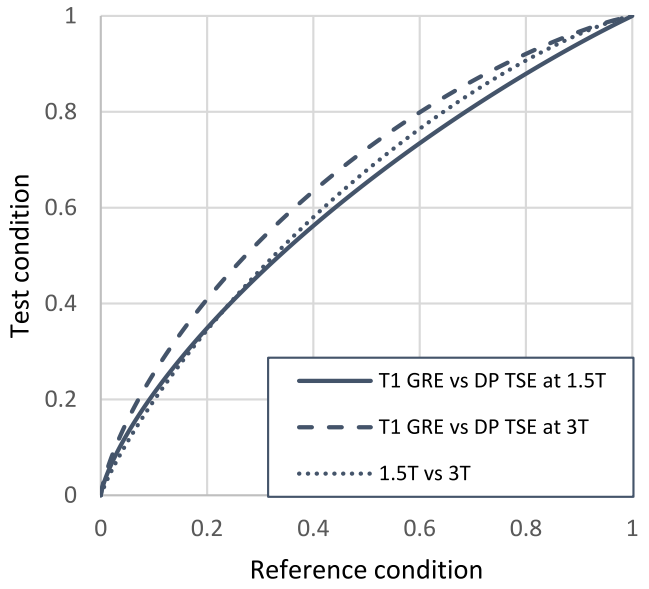


**Fig. 5.** Mean values of VGC Curves generated to compare: 1) T1 GRE sequence (reference condition) versus DP TSE sequence (test condition) at 1.5 T, 2) T1 GRE sequence (reference condition) versus DP TSE sequence (test condition) at 3 T, and 3) 1.5 T field strength sequences (reference condition) versus 3 T field strength sequences (test condition).

visibility in a coronal view [26]. Theoretically, lower limb internal or neutral position has no impact on prosthesis sizing and fitting as 3D images were acquired, nonetheless, the coronal view can influence the observer perception. Interestingly, trabecular and cortical bone differentiation was always scored as defined, which overcomes the main weak point of MRI compared to the X-ray-based machines to reproduce the bone structure and differentiation, which is essential for sizing and templating the total hip prosthesis [7].

VGC analysis results are aligned with the VGA analysis and 3D DP TSE sequences should be preferred over 3D T1 GRE. Moreover, image acquisition with high-resolution should ideally be performed at 3 T rather than 1.5 T field strength, which allows to better fulfil IQ requirements. Finally, 3D DP TSE at 3 T resulted as the best sequence to reproduce anatomical references with adequate IQ for THA preoperative planning. These results are expected as DP sequences compared to T1 sequences, TSE compared to GRE and 3 T compared to 1.5 T provide better SNR and indirectly better anatomical reproduction [15]. Nevertheless, Ultra-short Echo Time (UTE) or Zero Echo Time (ZTE) sequences seem to be promising for anatomical reproduction, especially for cortical bone evaluation [43,44]. However, these new sequences have a long acquisition time and were not included in this study. Artificial intelligence could be useful to solve UTE and ZTE long acquisition time problems to acquire high-resolution data [40–42].

ICC results are acceptable but the difficulty in evaluating noisy images and the differences in perception and preferences of the observers probably led to a reduced ICC [21]. Furthermore, no precise reference point was indicated to evaluate criteria, which could increase scoring variability and decrease ICC value [21]. As the correlation and agreement between observers is not perfect and the k statistics is affected by disagreement, it explains the low PABAK results of this study [27].

Some limitations were identified in this study. At first, the sample did not have pathologies as this was a pilot study. It is recommended to recruit real patients in a larger scale study with pathology affecting the anatomical reproduction to evaluate any complications or limitations impairing the correct preoperative planning. Additionally, protocols could have been further optimised to evaluate if a reduced acquisition time sequence could lead to acceptable images for the purpose of the study. Only 3D high-resolution sequences have been tested in this case and comparison with 2D high-resolution sequences should be performed to evaluate feasibility to reduce acquisition time. The machines utilised in the study allowed for parallel imaging such as GRAPPA and Sense for time reduction, however they were not equipped with last advanced technology such as compressed sensing, artificial intelligence which allow to further enhance IQ and reduce acquisition time.

The main limitation for the perceptual visual assessment is the lack of reference points used by the observers for the interpretation of IQ and anatomical reproduction, this can lead to higher levels of intra and inter observers' variability. New studies with reference points to evaluate the images, especially in cross-sectional images can help to reduce variability between observers. New studies with reference points to evaluate the images, especially in cross-sectional images can help to reduce variability between observers. Further studies should be carried out to include Orthopaedic surgeons specialised in THA in the visual assessment of the images. Bone density cartography obtained with MRI should be further investigated to evaluate the accuracy of MRI compared to CT for bone structures. Finally, this exploratory study confirmed the feasibility of 3D MRI sequences for planning THA surgeries. No comparison of MRI images against 2D X-ray or CT images was performed nor was any evaluation of whether MRI could be used in real-time navigated THA surgery.

## 5. Conclusions

Our study shows that short-time MRI sequences have a potential added value for planning THA surgeries. 3D DP TSE and 3D T1 GRE sequences at 3 Tesla and 3D DP TSE at 1.5 Tesla scans presented an adequate anatomical reproduction and IQ required to size and fit a hip prosthesis after considering variable age, height, weight, and BMI. Future studies should consider a wider population with pathological variations for clinical validation. Furthermore, other sequences such as ultra-short echo time (UTE) and artificial intelligence should be investigated to optimise the protocol and reduce acquisition time.

## Funding

This research did not receive any specific grant from funding agencies in the public, commercial, or not-for-profit sectors.

## CRediT authorship contribution statement

**Switinder Singh Ghotra:** Writing – original draft, Visualization, Validation, Project administration, Methodology, Investigation, Formal analysis, Conceptualization. **Yann Cottier:** Writing – review & editing, Resources, Methodology, Investigation, Conceptualization. **Christine Bruguier:** Writing – review & editing, Resources, Methodology, Investigation. **Alejandro Dominguez:** Writing – review & editing, Resources, Investigation. **Pascal Monnin:** Writing – review & editing, Supervision. **Cláudia Sá dos Reis:** Writing – review & editing, Visualization, Supervision, Resources, Methodology, Conceptualization.

## Declaration of competing interest

The authors declare that they have no known competing financial interests or personal relationships that could have appeared to influence the work reported in this paper.

## References


[1] Swiss National Joint Registry. SIRIS Report 2019. Siris [Internet]. 2019;88. Available from: https://www.researchgate.net/publication/337533256_SIRIS_Report_2019_Annual_Report_of_the_Swiss_National_Joint_Registry_Hip_and_Knee_2012_-_2018.

[2] L.K. King, L. March, A. Anandacoomarasamy, Obesity Osteoarthr. 63 (August) (2013) 185–193.

[3] S.C. Wearing, E.M. Hennig, N.M. Byrne, J.R. Steele, A.P. Hills, Musculoskeletal disorders associated with obesity: A biomechanical perspective, Obes. Rev. 7 (3) (2006) 239–250.

[4] Omar MF, Nafe WM. Orthopedic & muscular system: current research total hip replacement in patients younger than thirty years 7-10 years follow up. 2016;5(4): 10–13.

[5] M. Moralidou, A. Di Laura, J. Henckel, H. Hothi, A.J. Hart, Three-dimensional preoperative planning of primary hip arthroplasty: a systematic literature review, EFORT Open Rev. 5 (12) (2020) 845–855.

[6] Huppertz A, Radmer S, Asbach P, Juran R, Schwenke C, Diederichs G, et al. Eur. J. Radiol. 2009;EURR 4622.

[7] A. Huppertz, S. Radmer, M. Wagner, T. Roessler, B. Hamm, M. Sparmann, Computed tomography for preoperative planning in total hip arthroplasty: What radiologists need to know, Skeletal Radiol. 43 (8) (2014) 1041–1051.

[8] Colucci PG, Chalmers BP, Miller TT. Imaging of the Hip Prior to Replacement: What the Surgeon Wants to Know. Semin Ultrasound, CT MRI [Internet]. 2023;44 (4):240–51. Available from: DOI: 10.1053/j.sult.2023.02.001.

[9] IAEA, Implications for occupational radiation protection of the new dose limit for the lens of the eye, Int. Energy Agency 1731 (1731) (2013).

[10] G. Zeng, F. Schmaranzer, C. Degonda, N. Gerber, K. Gerber, M. Tannast, et al., MRI-based 3D models of the hip joint enables radiation-free computer-assisted planning of periacetabular osteotomy for treatment of hip dysplasia using deep learning for automatic segmentation, Eur. J. Radiol. Open [internet] November 2020 (8) (2021) 100303. Available from: DOI: 10.1016/j.ejro.2020.100303.

[11] O.A. Behery, L. Poultsides, J.M. Vigdorchik, Modern imaging in planning a personalized hip replacement and evaluating the spino-pelvic relationship in prosthetic instability, Pers. Hip. Knee Jt. Replace (2020) 143–156.

[12] M.C. Florkow, K. Willemsen, F. Zijlstra, W. Foppen, B.C.H. van der Wal, J.R.N. van der Voort van Zyp, et al., MRI-based synthetic CT shows equivalence to conventional CT for the morphological assessment of the hip joint, J. Orthop. Res. 40 (4) (2022) 954–964.

[13] A. Naraghi, L.M. White, Three-dimensional MRI of the musculoskeletal system, Am. J. Roentgenol. 199 (3) (2012) 283–293.

[14] J. Fritz, R. Guggenberger, F. Del Grande, Rapid musculoskeletal MRI in 2021: clinical application of advanced accelerated techniques, Am. J. Roentgenol. 216 (3) (2021) 718–733.

[15] Kastler B., Vetter D. Comprendre l ' IRM. 2018.

[16] L. Shapiro, M. Harish, B. Hargreaves, E. Staroswiecki, G. Gold, Advances in musculoskeletal MRI – Technical considerations, Available from, Bone [internet] 23 (1) (2008) 1–7, https://www.ncbi.nlm.nih.gov/pmc/articles/PMC3624763/pdf/nihms412728.pdf.

[17] F. Del Grande, R. Guggenberger, J. Fritz, Rapid musculoskeletal MRI in 2021: Value and optimized use of widely accessible techniques, Am. J. Roentgenol. 216 (3) (2021) 704–717.

[18] Bath M. Viewdex: A Status Report. 2016;169(1):38–45.

[19] A. Svalkvist, S. Svensson, T. Hagberg, M. Båth, Viewdex 3.0 - Recent development of a software application facilitating assessment of image quality and observer performance, Radiat. Prot. Dosim. 195 (3–4) (2021) 372–377.

[20] S. Börjesson, M. Håkansson, M. Båth, S. Kheddache, S. Svensson, A. Tingberg, et al., A software tool for increased efficiency in observer performance studies in radiology, Radiat. Prot. Dosim. 114 (1–3) (2005) 45–52.

[21] Precht H, Hansson J, Outzen C, Hogg P, Tingberg A. Radiographers' perspectives' on Visual Grading Analysis as a scientific method to evaluate image quality. Radiography [Internet]. 2019;25:S14–8. Available from: DOI: 10.1016/j.radi.2019.06.006.

[22] M. Båth, L.G. Månsson, Visual grading characteristics (VGC) analysis: A non-parametric rank-invariant statistical method for image quality evaluation, Br. J. Radiol. 80 (951) (2007) 169–176.

[23] L.G. Mansson, Methods for the evaluation of image quality: A review, Radiat. Prot. Dosim. 90 (1–2) (2000) 89–99.

[24] Sharma A. Efficacy of conventional method of preoperative templating in implant size selection in patent undergoing total hip arthroplasty Efficacy of conventional method of preoperative templating in implant size selection in patent undergoing total hip arthroplas. 2020;(January).

[25] Shaikh AH. Preoperative Preoperative Planning Planning of of Total Total Hip Hip Arthroplasty Arthroplasty. :3–18.

[26] A. Colombi, D. Schena, C.C. Castelli, Total hip arthroplasty planning, EFORT Open Rev. 4 (11) (2019) 626–632.

[27] H. Precht, O. Gerke, K. Rosendahl, A. Tingberg, D. Waaler, Digital radiography: optimization of image quality and dose using multi-frequency software, Pediatr. Radiol. 42 (9) (2012) 1112–1118.

[28] T.K. Koo, M.Y. Li, A guideline of selecting and reporting intraclass correlation coefficients for reliability research, Available from: J. Chiropr. Med. [internet] 15 (2) (2016) 155–163, https://doi.org/10.1016/j.jcm.2016.02.012.

[29] G. Chen, P. Faris, B. Hemmelgarn, R.L. Walker, H. Quan, Measuring agreement of administrative data with chart data using prevalence unadjusted and adjusted kappa, BMC Med. Res. Method. 9 (1) (2009) 1–8.

[30] J.R. Landis, G.G. Koch, The measurement of observer agreement for categorical data, Biometrics 33 (1) (1977) 159.

[31] Bath M. Evaluating imaging systems : practical applications. 2010;139(1):26–36.

[32] M. Bath, J. Hansson, Vgc analyzer : a SoftwAre for statistical analysis of fully crossed multiple-reader multiple-case visual grading characteristics studies, Radiat. Prot. Dosim. 1–8 (2016).

[33] J. Hansson, L.G. Månsson, M. Båth, Evaluation of VGC analyzer by comparison with gold standard ROC software and analysis of simulated visual grading data, Radiat. Prot. Dosim. 195 (3–4) (2021) 378–390.

[34] J. Hansson, M. Ba, Vgc analyzer : a Softw are for statistical analysis of fully crossed multiple-reader multiple-case, Radiat. Prot. Dosim. 169 (1) (2016) 1–8.

[35] L.R. Chong, K. Lee, F.Y. Sim, 3D MRI with CT-like bone contrast – An overview of current approaches and practical clinical implementation, Eur. J. Radiol. 143 (2021 Oct) 109915.

[36] T.D. Lerch, C. Degonda, F. Schmaranzer, I. Todorski, J. Cullmann-Bastian, G. Zheng, et al., Patient-specific 3-D magnetic resonance imaging-based dynamic simulation of hip impingement and range of motion can replace 3-D computed tomography-based simulation for patients with femoroacetabular impingement: implications for planning open hip preserv, Am. J. Sports Med. 47 (12) (2019) 2966–2977.

[37] M.S. Mak, J. Teh, Magnetic resonance imaging of the hip: Anatomy and pathology, Polish. J. Radiol. 85 (1) (2020) e489–e508.

[38] O.M. Abdulaal, L. Rainford, P.J. MacMahon, P. Kenny, F. Carty, M. Galligan, et al., Evaluation of optimised 3D turbo spin echo and gradient echo MR pulse sequences of the knee at 3T and 1.5T, Radiography [internet] 27 (2) (2021) 389–397. Available from: DOI: 10.1016/j.radi.2020.09.020.

[39] F. Del Grande, N. Hinterholzer, D. Nanz, 3D MRI: technical considerations and practical integration, Semin. Musculoskelet. Radiol. 25 (3) (2021 Jun) 381–387.

[40] A.S. Chaudhari, Z. Fang, F. Kogan, J. Wood, K.J. Stevens, E.K. Gibbons, et al., Super-resolution musculoskeletal MRI using deep learning, Magn. Reson. Med. 80 (5) (2018) 2139–2154.

[41] N. Gorelik, S. Gyftopoulos, Applications of artificial intelligence in musculoskeletal imaging: from the request to the report, Can. Assoc. Radiol. J. 72 (1) (2021) 45–59.

[42] S. Gyftopoulos, D. Lin, F. Knoll, A.M. Doshi, T.C. Rodrigues, M.P. Recht, Artificial intelligence in musculoskeletal imaging: current status and future directions, Am. J. Roentgenol. 213 (3) (2019) 506–513.

[43] S. Mastrogiacomo, W. Dou, J.A. Jansen, X.F. Walboomers, Magnetic resonance imaging of hard tissues and hard tissue engineered bio-substitutes, Mol. Imag. Biol. 21 (6) (2019) 1003–1019.

[44] E. Chang, J. Du, C.B. Chung, UTE imaging in the musculoskeletal system eric, J. Magn. Reson. Imaging 41 (4) (2015) 870–883.